
Accuracy of $Q_{\text{VEM}}^{\text{Peak}}$ fit for UB and UUB

Mauricio Suárez-Durán and Ioana C. Mariş

Université Libre de Bruxelles, Belgium

Abstract

From the deployment of the Upgraded Unified Board (UUB) it is expected to have a better accuracy for the calculation of the $Q_{\text{VEM}}^{\text{Peak}}$ values, respect of the previous Unified Board (UB). Here, a method to calculate the accuracy of the $Q_{\text{VEM}}^{\text{Peak}}$ values for the UUB and UB is presented, including a new method to fit the muon hump in charge calibration histogram. In this way, the accuracy was calculate for 75 UUB stations, and their respective UB version.

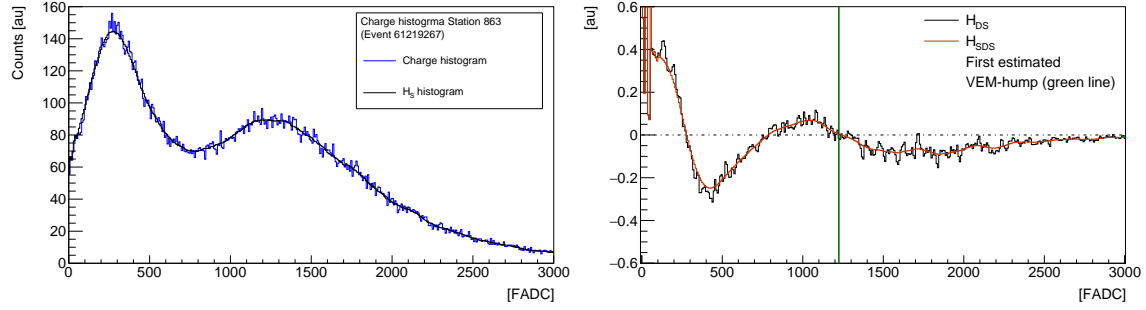


Figure 1: Algorithm to fit the muon hump in calibration charge histograms (see details in the text). Left: a sample of a typical charge calibration histogram, the black line represents the smoothing histogram after applying a 15-bin sliding window (H_S). Right: in black the first derivative histogram (H_{DS}) and its respective smoothing in red (H_{SDS}). Here, the green vertical line shows the maximum or the first approach for Q_{VEM}^{Peak} .

1 Introduction

The deployment of the Upgraded Unified Board (UUB) for the surface array [1] requires a systematic monitoring and calibration, using as reference the previous Unified Board (UB). The Q_{VEM}^{Peak} is one of the more important quantities to calculate and monitoring because it is used to normalize the SD signals, making possible the comparison among different WCDs, and also to understand the signals fluctuations [2].

In this work, the accuracy of the Q_{VEM}^{Peak} is calculated as a checker of its stability, extracting its value through fitting the muon hump in the charge calibration histograms [3] and comparing between UB and UUB. In order to guarantee the precision in this calculation, two methods have been implemented, first one regarding the fitting of the muon hump, and second one to chose a time window of seven days in a row which the fitted Q_{VEM}^{Peak} values were stable, in both version UB and UUB.

2 Fitting the muon hump

The Q_{VEM}^{Peak} value is obtained from charge calibration histograms by fitting the muon hump. We have implemented an algorithm which uses the first derivative to perform this fit, obtaining in this way a first approach of the hump position, and from there the fitting range. The figure 1 illustrated this algorithm, which detailed next:

1. Smoothing the histogram using a 15-bin sliding window, H_S .
2. Obtaining the first derivative from H_S , applying

$$\frac{f(x+1) - f(x-1)}{2h}, \quad (1)$$

and named as H_{DS} .

3. Smoothing H_{DS} , by 15-bin sliding window, and getting H_{SDS} .
4. Searching for the estimated Q_{VEM}^{Peak} , i.e. first bin for H_{SDS} equal to zero, from right to left.
5. Fixing the fitting range using n-bin leftward and n-bin rightward from the estimated Q_{VEM}^{Peak} .

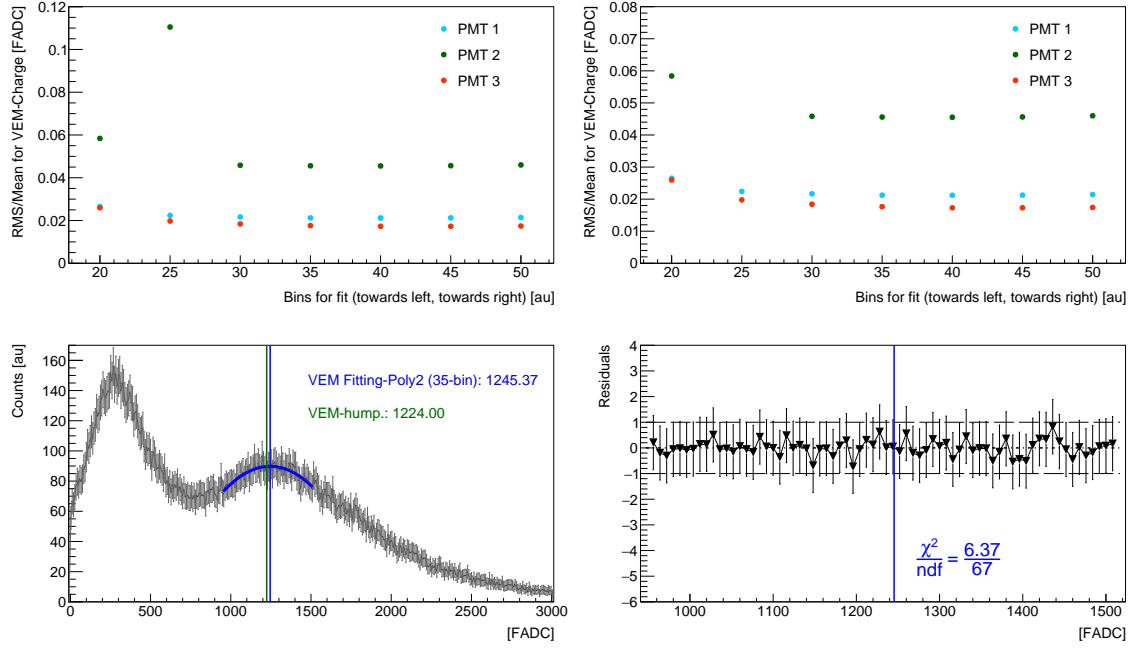


Figure 2: Top row, results for fitting stability of the hump muon, $\text{RMS}/\langle Q_{\text{VEM}}^{\text{Peak}} \rangle$, as function of the n-bin. After 30 bins the stability is reached. Bottom row, an example of application of the algorithm; here the vertical green line shows the hump VEM obtained from the first derivative (step 4.), and the vertical blue line shows the $Q_{\text{VEM}}^{\text{Peak}}$ obtained as the maximum of the fitted second order polynomial.

The last step in the algorithm requires an extra procedure in order to fixed the number of n-bin. So, a set of histograms have been fitted using different values for n, and then the stability of the fit, $\text{RMS}_n/\langle Q_{\text{VEM},n}^{\text{Peak}} \rangle$, have been checked; avoiding to fit the valley of the histogram. The results of this procedure are presented in figure 2. There, the stability of the fit is reached after 30-bin, which chosen as the number of n-bin for the step 5 of the algorithm. In the bottom row of the same figure, an example of applying this procedure is presented.

3 Sliding window algorithm for $Q_{\text{VEM}}^{\text{Peak}}$ accuracy calculation

The calculation of the accuracy is based on the selection of a period of time in which the $Q_{\text{VEM}}^{\text{Peak}}$ as a function of time was stable, in this case we have chosen a full week (7-day-row). To determine this time window, we have used the charge calibration histograms measured from August to November, 2021 for UUB and 2018 for UB. From these set of data, the average of $Q_{\text{VEM}}^{\text{Peak}}$ per day was plotted as function of time for each one of the 75, UUB and UB.

In order to chose the respective 7-day-row with a good statistic, a first condition was set in terms of the minimum of $Q_{\text{VEM}}^{\text{Peak}}$ values per day needed in each day. To apply this condition, the distribution of $Q_{\text{VEM}}^{\text{Peak}}$ per day was calculate, and it is presented in figure 3, from which we have chosen as 10 the minimum of $Q_{\text{VEM}}^{\text{Peak}}$ values per day.

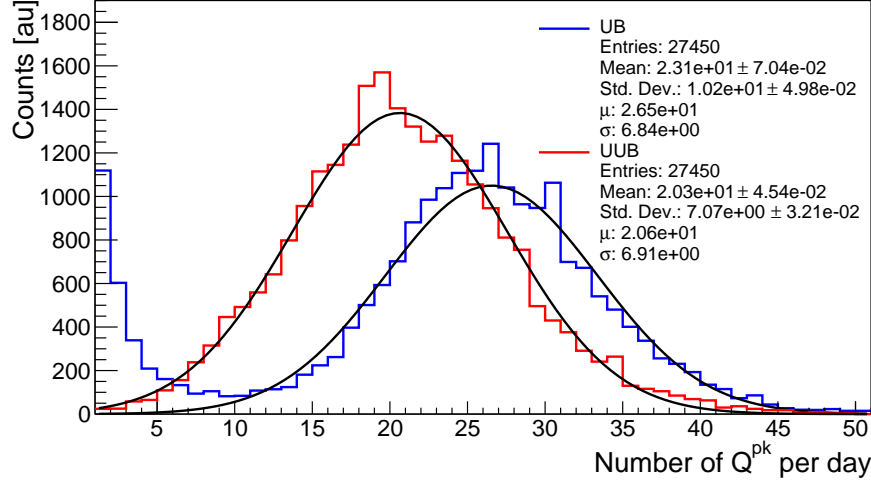


Figure 3: Distribution of $Q_{\text{VEM}}^{\text{Peak}}$ per day for 75 stations, from August to November, with UUB (red, year 2021) and UB (blue, year 2018) electronics version. The black line represents the respective Gaussian fit.

The sliding window algorithm was applied to each station, and each PMT, following next steps:

1. The $\langle Q_{\text{VEM}}^{\text{Peak}} \rangle$ per day as function of time is calculate from August to November. 2
2. Starting from the first day of August, a [7-day-series]₀ is build.
3. A check for continuity is applied, i.e. if each day has not more then 10 $Q_{\text{VEM}}^{\text{Peak}}$ values, or the 7 days are not consecutive (some day has not data), a new series is built, e.g. if series i has a discontinuity in day 3 jumping to day 5, a new 7-day-series is calculated from day 5. 4
6
4. If [7-day-series] _{i} is consecutive, a linear fit is applied, and the respective slope and p-value are stored. 8

The figure 4 shows the distribution for the p-values as function of the normalized slope (respect the average of the $Q_{\text{VEM}}^{\text{Peak}}$ during the 7 days), obtained by applying the former algorithm to the 75 stations, all PMTs. There, it is seen how the normalized slope is closer to zero for UB than UUB, whereas for both version the $\log_{10}(\text{p-value})$ distribution has a hot spot for values bigger than -4 . 10
12

With these results, and taking into the account that the number of degree of freedom is 5 for all the fits¹, we chose all fits matching with: $\chi^2 < 10$, i.e. $\log_{10}(\text{p-value}) < -1.12$, and a normalized slope between $\mu \pm \sigma$ (x axis, figure 4). The results after these cuts are presented in figure 5, where the distribution of the normalized slope is presented for both UB and UUB. With these results, we can chose the best 7-day-row to perform the accuracy calculation. 14
16
18

¹Here, only fits with 5 DOF were used; different ones were rejected.

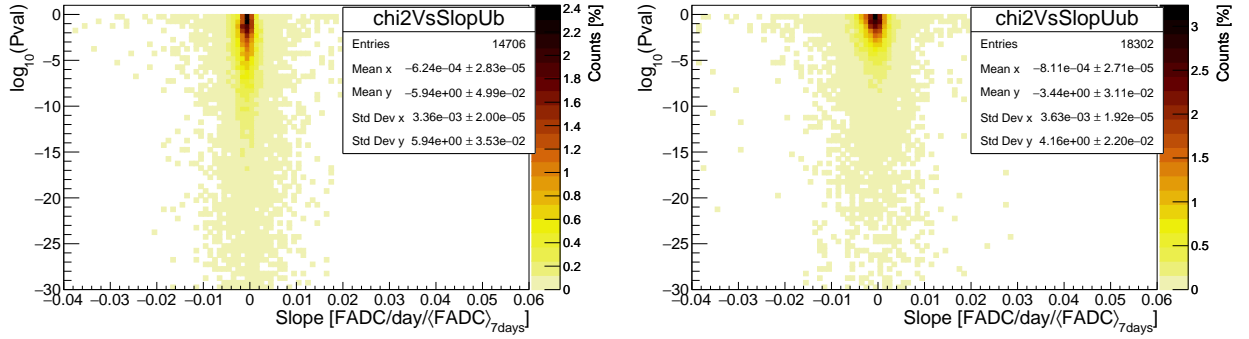


Figure 4: Distribution of p-value as function of the normalized slope (i.e. divided by the average of the $Q_{\text{VEM}}^{\text{Peak}}$ during the 7 days). Values obtained after applied the sliding window method to 75 stations, all PMT (see text for details). On the left the distribution for UB, and on the right the one for UUB. A hot spot for p-values bigger than -4 is observed for UB and UUB, whereas the normalized slope closer to zero for UB than UUB.

4 Accuracy calculation

The calculation for the $Q_{\text{VEM}}^{\text{Peak}}$ accuracy to each station was perform following the next steps for each station, for both UB and UUB version: 2

1. The best 7-day-row is chosen per PMT as the one with the normalized slope closest to zero and $\log_{10}(\text{p-value}) < -1.12$. 4
2. If for a certain station, either UB or UUB, some PMT has not a 7-day-row in agreement with the previous requirements, this PMT is remove for the calculation from both UB and UUB. 6
3. To each PMT, a singular normalized distribution of the respective $Q_{\text{VEM}}^{\text{Peak}}$ values is built; into the respective. 8
4. A Gaussian function is fitted to each PMT normalized distribution and then the accuracy is calculated as: σ/μ , respectively. 10

An example of the steps 3 and 4 of this method are illustrated in figure 6 for UB and UUB. There, it is possible to see that the distribution of the normalized $Q_{\text{VEM}}^{\text{Peak}}$ values fits to a Gaussian function, for the both versions. 14

16

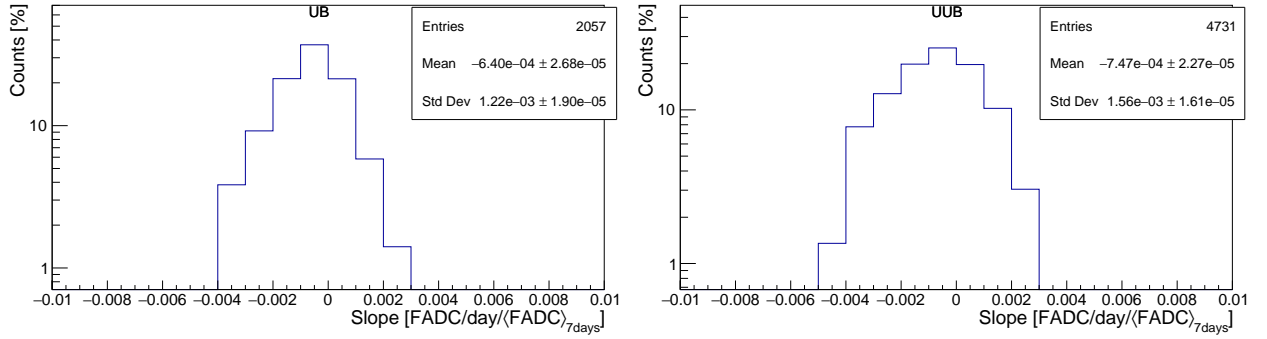


Figure 5: Distribution of normalized slopes fitted for $[7\text{-days-row}]_i$ matching: $\chi^2 < 10$ ($\log_{10}(\text{p-value}) > -1.12$), and normalized slope $\mu \pm \sigma$ (x axis, figure 4). For UB case, the mean of the distribution is closer to zero than UUB case.

The results for the $Q_{\text{VEM}}^{\text{Peak}}$ accuracy are presented in figure 7, where the accuracy per station is presented on the left, whereas the its distribution is showed on the right panel. There, it is seen that the accuracy for UUB takes a value of $1.61\% \pm 0.06\%$, and $1.36\% \pm 0.06\%$ for UB. The latest value differ from the 2% calculated in [4] for the engineering array.

On the other hand, in figure 8 the difference between the accuracy for UB minus the one for UUB is presented per station, left plot, together its distribution, right plot. There, it is possible to confirm that the $Q_{\text{VEM}}^{\text{Peak}}$ accuracy for UUB stations are in general bigger than the ones for UBs, with a mean value for this difference of $-0.252\% \pm 0.052\%$.

Examples of outliers in figure 7, and in figure 8 are presented in figures 9 and 10, respectively.

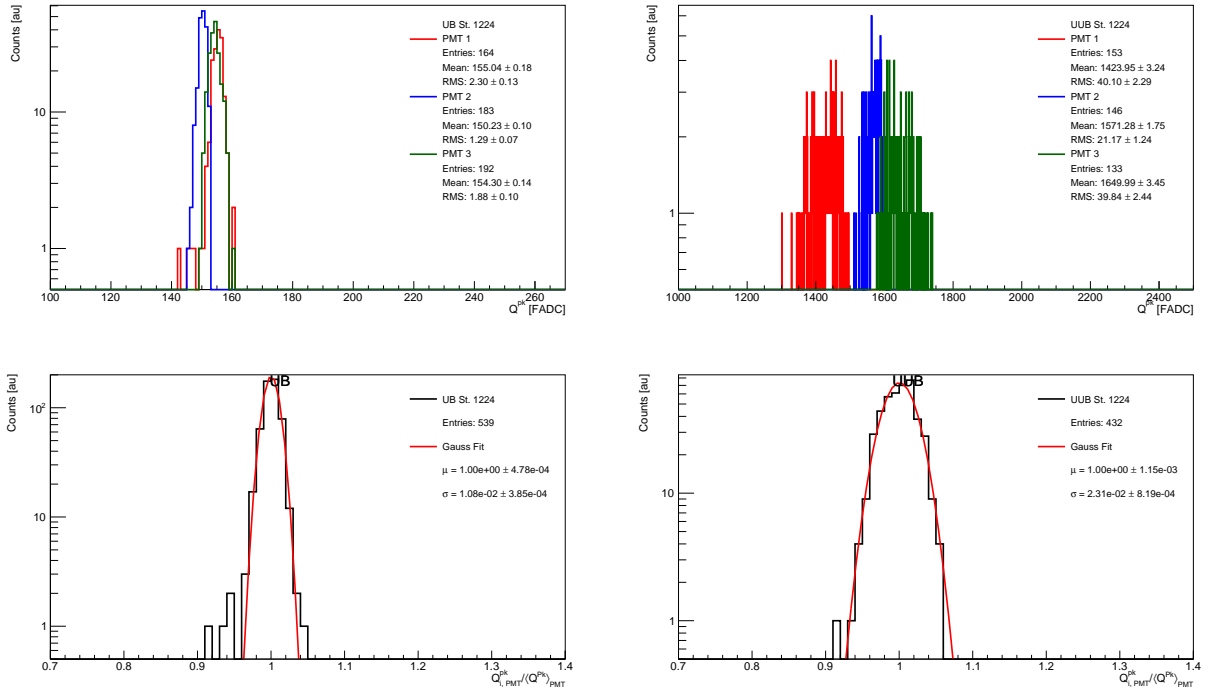


Figure 6: Example of the method applied to calculate the accuracy of the Q_{VEM}^{Peak} , station 1224. Upper row, distribution of the Q_{VEM}^{Peak} values from the best 7-day-row selected; left UB, right UUB. Lower row, former distribution normalized respect the average of the respective PMT. The red line represents the Gauss function fitted.

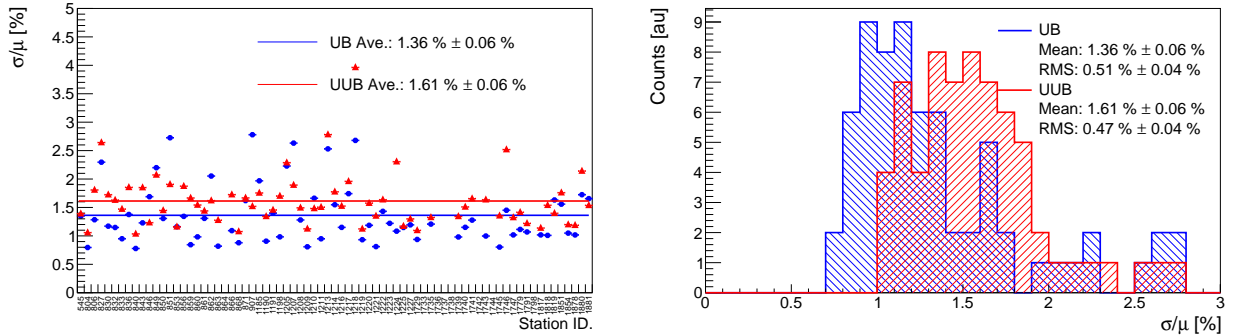


Figure 7: Results for the accuracy calculation of the Q_{VEM}^{Peak} fitting, using the algorithm describe in section 3; in blue color for UB, and in red color for UUB. In the right side, the distribution of the σ/μ values is presented for both version, UUB (red) and UB (blue). Here, it is possible to see that the accuracy for UUB is better than the one for UB.

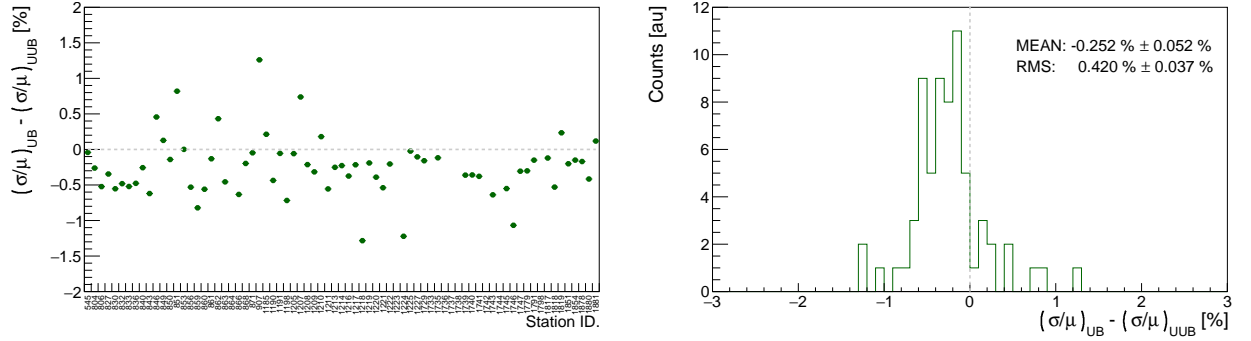


Figure 8: Difference between the accuracy for UB minus the one for UUB. Left, the plot of this difference per station. Right, its distribution. Here, it is possible to see how per UB stations the accuracy is lower than the one for the respective UUB version.

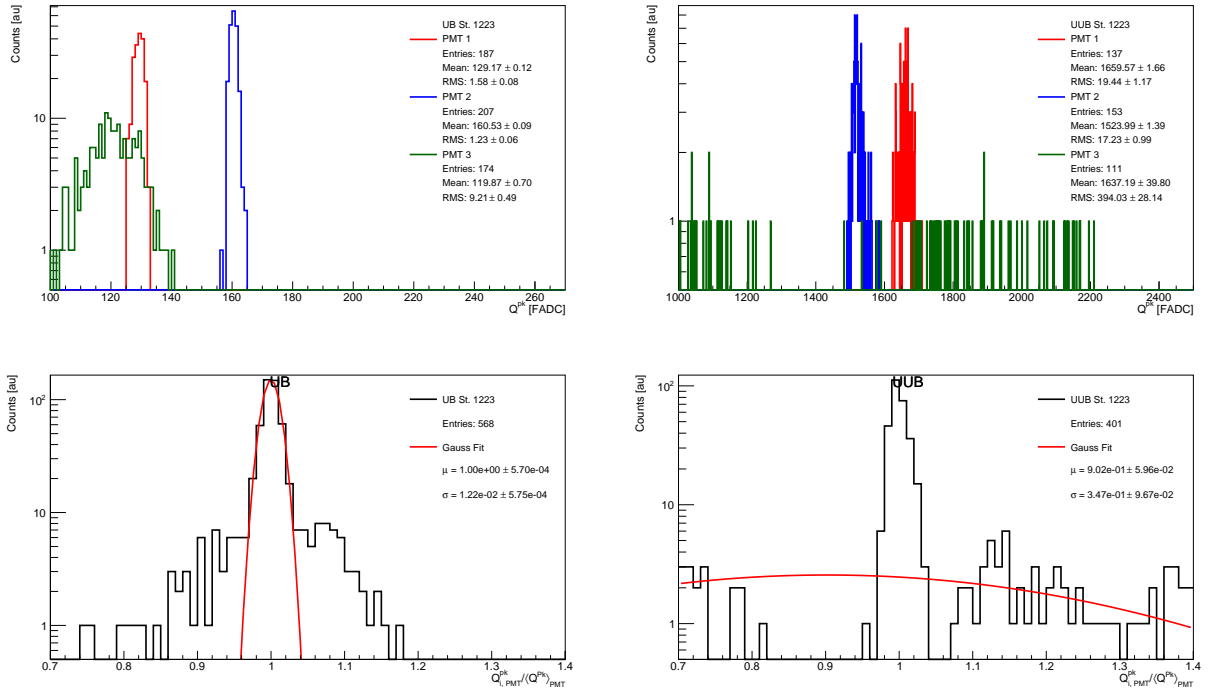


Figure 9: Station 1223 with an outlier accuracy ($> 10\%$). Here, it is possible to see how the PMT3 produce a wide distribution for the normalized Q^{Peak}_{VEM} .

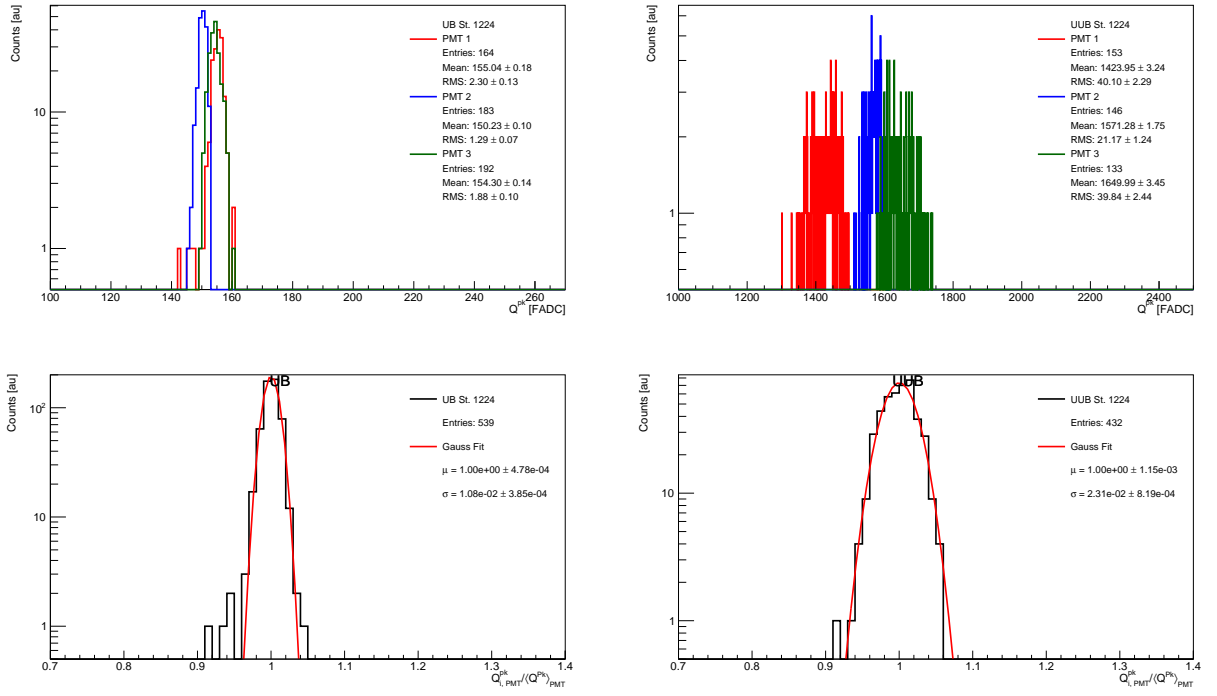


Figure 10: Station 1224 with an outlier value for the difference between accuracy UB minus accuracy UUB ($< -1\%$). Here, it is seen that the normalized distribution of the $Q^{\text{Peak}}_{\text{VEM}}$ values is wider in the UUB version than in UB one.

5 Summary and conclusions

We have developed and presented a different method to fit the muon hump in charge calibration histograms, and from there to estimate the respective $Q_{\text{VEM}}^{\text{Peak}}$ value, for UUB and UB version; as it was presented in figures 1 and 2. 2
4

A sliding window method was implemented to find the most stable period for the $Q_{\text{VEM}}^{\text{Peak}}$ values, i.e. during 7 consecutive days in a row; for both version, UB and UUB. 6
8

We have calculate the accuracy of the $Q_{\text{VEM}}^{\text{Peak}}$ using the normalized distribution of the $Q_{\text{VEM}}^{\text{Peak}}$ values for the most stable period. From there, we have calculated the accuracy for UUB version as $1.61 \% \pm 0.06 \%$, and $1.36 \% \pm 0.06 \%$ for UB, which differ from the 2 % calculated in [4] for the engineering array. 10
12

References

- [1] A. Aab *et al.*, "The Pierre Auger Observatory Upgrade - Preliminary Design Report," 14
arXiv:1604.03637 [astro-ph.IM].
- [2] M. Ave, P. Bauleo, T. Yamamoto, *Signal Fluctuation in the Auger Surface Detector Array*, GAP 16
2003-030
- [3] X. Bertou and P.S. Allison and C. Bonifazi and *et al.*, *Calibration of the surface array of the* 18
Pierre Auger Observatory, Nuclear Instruments and Methods in Physics Research Section A:
Accelerators, Spectrometers, Detectors and Associated Equipment, vol. 568, number 2, 2006 20
- [4] A. Tripathi, K. Arisaka, M. Healy, D. Barnhill, W. Slater, *A Systematic Calibration of Surface*
Detectors using Muon Data from the Engineering Array, GAP 2002-046 22